ESCUELA DE CONSTRUCCIÓN CIVIL
FACULTAD DE INGENIERÍA

Revista de la Construcción
Journal of Construction

Research Article

Numerical estimation of the subgrade reaction modulus of a horizontally loaded piled raft

Francisco Javier Alva García [1*], Liosber Medina García [2], Márcio Muniz de Farias [3]

1 INFRALAB, University of Brasilia (UnB), Brasilia (Brazil); fj_alva@icloud.com
2 Transport Engineering Department, Federal University of Goias, Goias (Brazil); lmedina@ufg.br
3 Department of Civil and Environmental Engineering, University of Brasilia, Brasilia (Brazil); muniz@unb.br
*Correspondence: fj_alva@icloud.com (F. Alva)

Received: 18.04.23; **Accepted:** 01.05.24; **Published:** 12.12.24

Citation: Alva, F., Medina, L., and Muniz de Farias, M. (2024). Numerical estimation of the subgrade reaction modulus of a horizontally loaded piled raft. Revista de la Construcción. Journal of Construction, 23(3), 538-553. https://doi.org/10.7764/RDLC.23.3.538

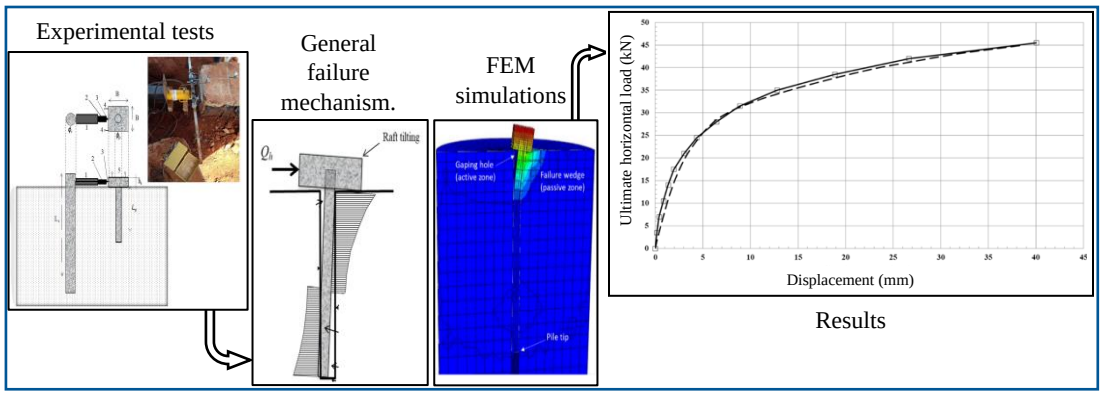

Highlights:

- Full-scale tests reveal large gaps between theory and reality, vital for model validation.
- Understanding internal force behavior in soil and piles depends on successful modeling.
- Reviewing foundation design differently avoids over-sizing, cutting costs, and saving resources.

Abstract: A horizontal full-scale test was executed in a piled raft with a single pile. Later, from those measured experimental results, some numerical simulations were carried out using a commercial software Abaqus 2019 obtaining acceptable approximations. During the numerical analysis, the elastic-plastic behavior of each material comprising the foundation system has been considered, including the soil, the concrete, and the steel. Based on such numerical approximations, a polynomial function $y = f(x)$ that represent the pile deflections along the pile shaft has been calculated and plotted. Later, from this function the rotation, the bending moments, the shearing forces, and the load intensity along the pile were estimated; also, the subgrade reaction modulus of the soil was computed, and some *p-y* curves at specific depth points are presented according to the numerical results. Finally, this paper allowed obtaining a clear idea about the behavior and distribution of the internal forces not only in the foundation soil but also in the pile, from a success numerical performance.

Keywords: Piled raft, horizontal load, soil-structure interaction, Abaqus numerical modeling.

Abbreviation:

B – raft width
c – undrained cohesion
CU – consolidated undrained
E_c – modulus of elasticity of the concrete
E_p – modulus of elasticity of the pile
E_s – undrained elastic modulus
E_{steel} – modulus of elasticity of the steel
FEM –finite element method
fck – characteristic compressive strength of concrete
f_s – shear strength
f_{yk} – characteristic yield strength of steel
γ_{nat} – natural unit weight of soil
γ_s – unit weight of steel
hr – raft height
Ip – moment of inertia of the pile section
k_o – coefficient of earth pressure
K – subgrade reaction modulus of soil
L_p – long pile
L_r – long reaction pile
MH – silty with high compressibility
ML – silty with low compressibility
ν – Poisson coefficient
Qh – ultimate load measured at field
SPT – standard penetration test
USCS – unified soil classification system
w – moisture content
y – lateral deflection of the pile along the length of the pile
ϕ – undrained friction angle
ϕ_p – pile diameter
ϕ_r – reaction pile diameter

1. Introduction

The concept of raft foundations enhanced with deep foundation elements, typically piles and therefore the name “piled rafts”, has received considerable attention in recent years. According to Patil et al. (2013), the piled raft system has emerged as a good alternative to the foundation-type system used for tall buildings. However, numerous piles are designed based on empirical models that overlook crucial soil properties. This oversight, particularly in areas with lateritic and collapsible soils, leads to over-dimensioned projects, escalating costs, and resource wastage (André de Almeida, Miguel, and Teixeira 2011).

The influence of lateral loads on the performance of these foundations systems has been studied by several authors using different numerical methods (Stacul et al., 2017; Deb and Pal, 2019; Abdel-Azim et al., 2020; García et al., 2020; Jeong et al., 2024). Lateral force resistance in a pile is complex and derived from three-dimensional processes. According whit Kim et al., (2011) these processes include: (1) passive lateral soil resistance along the leading face of the pile; and (2) shearing along the shaft perimeter. A thorough analysis of such a force system requires sophisticated three-dimensional numerical methods.

Theoretically, the problem of a pile subjected to lateral loading is represented by a fourth-order differential equation. The general solution to this equation results in the lateral displacements caused by the load applied at the top of the pile. A

solution to such a differential equation yields a set of curves, as shown in Figure 1. It should be highlighted that several assumptions were made in deriving this differential equation, and some simplifications were also made to solve it, mainly in the boundary conditions considered.

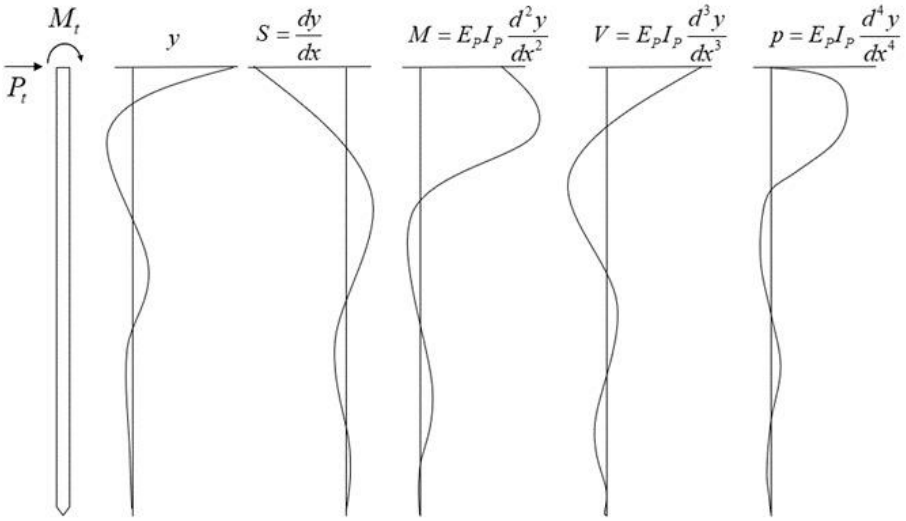

Figure 1. Form of the results obtained from a complete solution. (Reese and Van Impe, 2001).

These graphics have been obtained, in this study, by numerical modeling. In this paper, all considerations taken into account during the numerical work are discussed.

With the aim of investigating the internal distribution of forces both in the pile and in the soil dominium, a three-dimensional approach to analyzing the laterally loaded piled raft system is presented. The foundation consists of a piled raft with a single pile, which was subjected to a full-scale lateral load test, and an experimental horizontal ultimate load vs displacement (Q_h-y) curve has been obtained.

This paper is based on the full-scale experimental tests on piled raft systems under horizontal forces, (Alva 2017), in which is shown the experience gathered during the experimental phase of those tests, with a subsequent numerical calibration and post-experimental simulations. The piled raft foundation system was modeled through the finite element method (FEM), using Abaqus commercial software. These numerical simulations allowed the understanding of the phenomenon in terms of how the piled raft interact with the surrounding soil.

The novelty of this paper concerns studying the mechanical behavior of a concrete pile submitted to lateral loading; combining some full-scale measurements over the pile that were used in numerical modeling (FEM) along whit available theorical solutions resulted in interesting perspectives to be considered.

2. Materials and methods

The geotechnical profile of the FEC-UNICAMP research site (600 m^2 area) consists of a silty clay layer, which is porous, colluvial, lateritic and collapsible, overlying a brown silty sand layer with altered rocks. Figure 2 shows the profile obtained from Standard Penetration Test (SPT), plotting the N72% (average energy) SPT blow counts vs depth. Through those graphic results were defined four layers with the same properties.

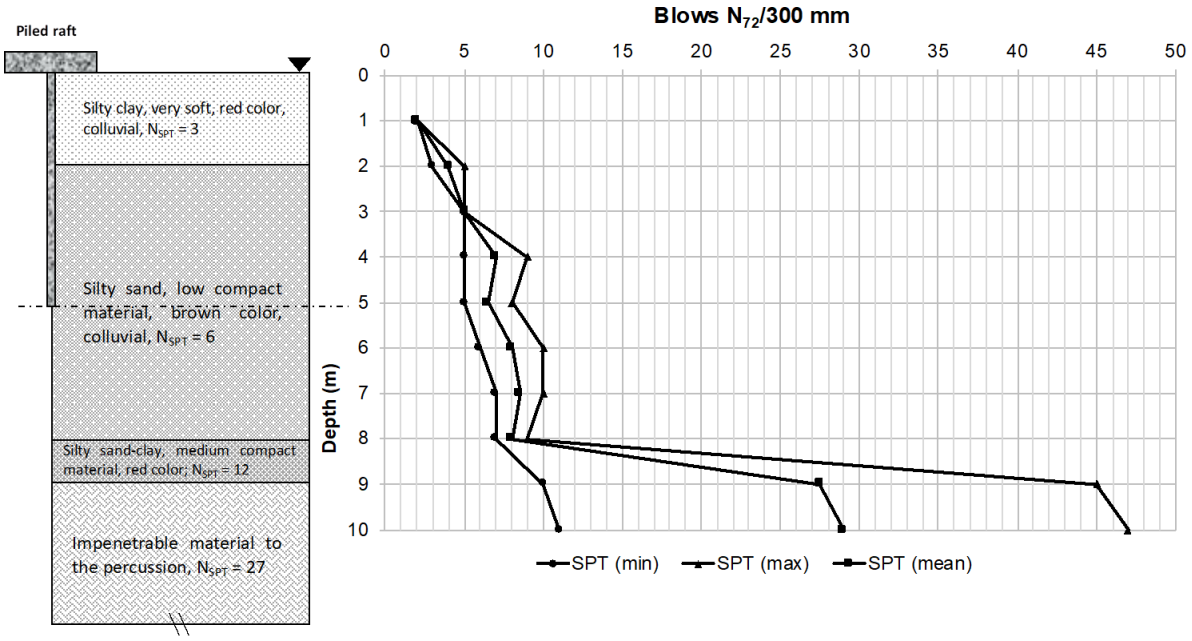

Figure 2. The SPT chart and simplified geological profile from the research site.

Laboratory results from physical characterization, consolidation, triaxial compression (type CU), permeability, normal Proctor compaction and suction tests were obtained by Gon (2011). Some geotechnical parameters of the soil are displayed in Table 1.

Table 1. Geotechnical parameters of the porous clay.

Laboratory testing results of the porous clay						
Depth (m)	USCS	γ_{nat} (kN/m^3)	w (%)	Es (MPa)	c (kPa)	ϕ (°)
1.00	MH	14.10	28.30	13.79	7.40	22.00
2.00	ML	14.20	27.90	11.43	7.85	21.00
3.00	ML	14.00	28.00	8.50	11.60	22.00
4.00	ML	14.40	25.50	11.49	5.75	23.00
5.00	ML	15.50	26.20	9.86	24.00	21.00
6.00	ML	15.30	26.10	19.95	42.40	22.00
7.00	ML	15.40	28.30	10.93	41.93	22.00
8.00	MH	15.20	32.30	11.01	26.40	22.00

USCS - Unified soil classification system: MH – Silty with high compressibility; ML – Silty with low compressibility; γ_{nat} - Natural unit weight; w – Moisture content; Es – Undrained elastic modulus; c – Undrained cohesion; ϕ – Undrained friction angle.

2.1. Experimental procedure

A horizontal load test was carried out on the piled raft named *CC1* foundation system, 5.0m in length and 0.25m in diameter, natural soil moisture conditions, and the bottom face of the raft had contact with the ground. The strength of the concrete used during construction was f_{ck}=20.0 MPa; in addition, CA-50 type steel of 10.0mm in diameter for the rods and steel stirrups (helical type) and of 6.5mm in diameter for reinforcement of the structures were used. These structural details are displayed in Figure 3. The field horizontal loading test was performed in accordance with the recommendations of Brazilian testing standard NBR12131 (ABNT 2006).

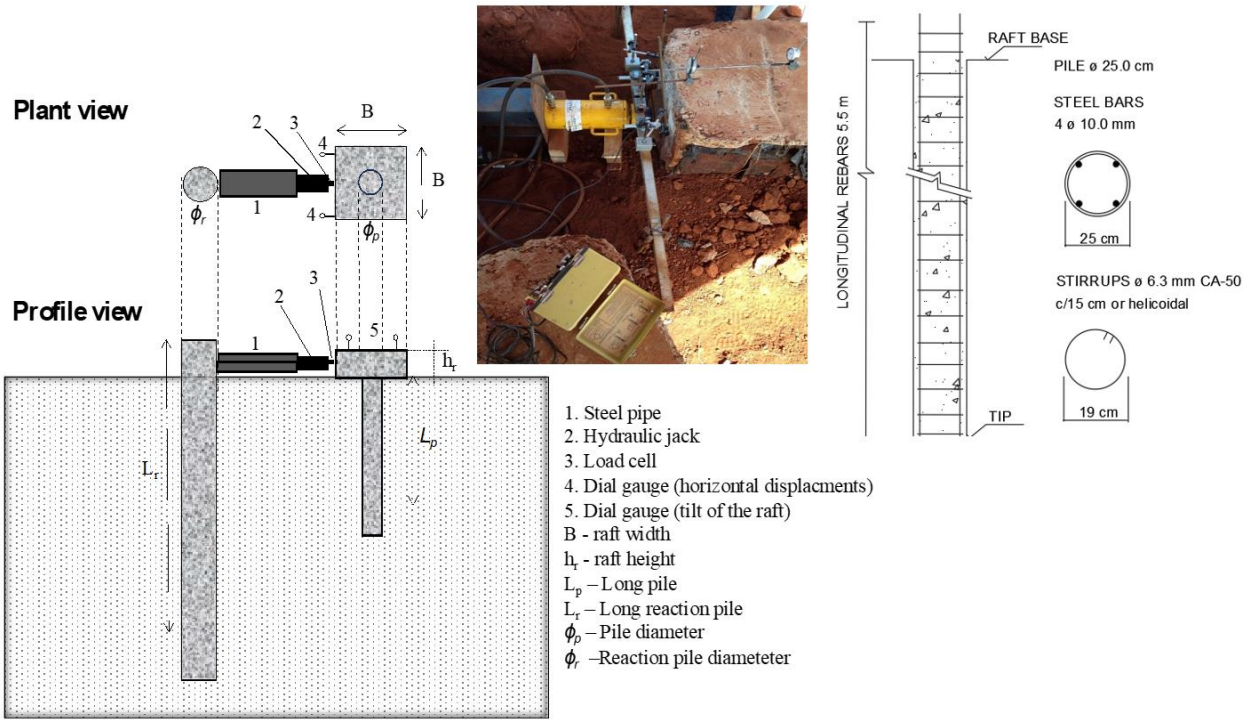

Figure 3. The structural details of the *CC1* piled raft system.

2.2. Modeling framework

A commercial software Abaqus based on the finite element modeling (FEM) has been used for the numerical analysis. The numerical model is composed of four parts: soil dominium, concrete raft, concrete pile, and steel reinforcement all displayed in Figure 4, and must be rich enough to be able to capture the important phenomenon, but it should not be more complex than necessary, since this would only increase the computer time needed. Furthermore, to be able to verify the quality of the models, numerical results must be compared to experimental results.

To obtain good numerical approximations, a sensitivity numerical analysis was carried out using different finite element types, geometry of the soil dominium, numerical integration type, meshing density, constitutive models, etc. Table 2 shows some data of such analysis.

Table 2. Element finite type selected.

Part	Element type	Number of elements
Soil (3D)	C3D8R	10.640
Pile (3D)	C3D6R	588
Raft (3D)	C3D8R	1752
Rebars (3D)	T3D2	751

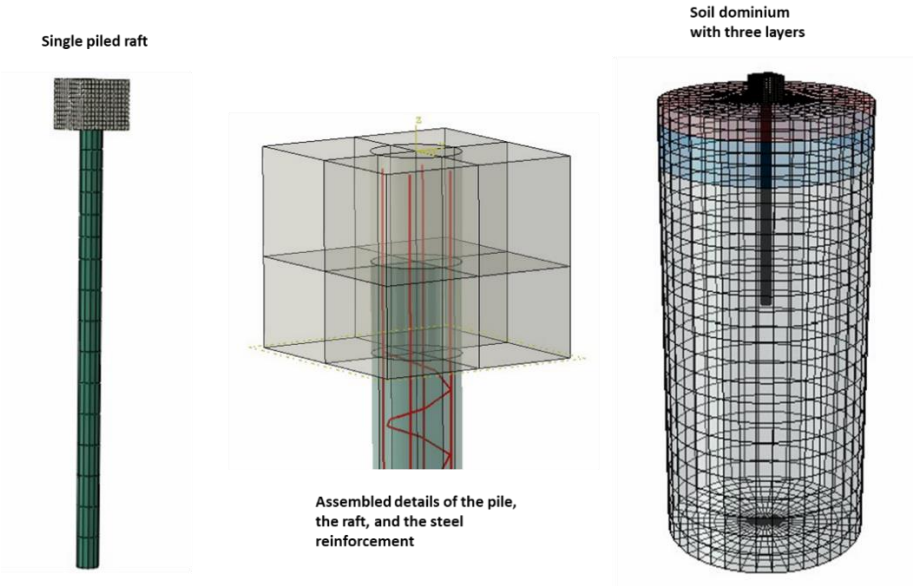

Figure 4. The all parts assembled in the numerical model.

2.3. Constitutive models

Has been assumed an elastic-plastic behavior for the concrete material, and the concrete damage plasticity constitutive model was considered, see the Abaqus User's Manual (2019) and Sümer and Aktaş, (2015) for the parameters required. The interaction between the raft and the pile was neglected, setting the contacts between both parts as tie type, according to the software. Although they are two different parts of the numerical model, its structural behavior is like a single element. The constitutive model used to simulate the steel reinforcement was the classical metal (von Mises) elastic-perfectly plastic model. With respect to the interface between the concrete material and the steel material, a perfect bonding between them has been assumed, setting as embedded region according to the software.

One of the main considerations for the soil material was to represent the soil dominium by the first three layers and discard all the rest, according to the laboratory data shown previously in Table 1. This decision was based on the fact that the horizontal loading has a depth influence between 3 to 5 times the diameter of the pile, Reese and Van Impe (2001), resulting in a depth of influence of around 1.25m. The geologic profile displayed in Figure 2 gives a clear overall idea of the position of the piled raft system embedded in the natural underground. Part of the soil surrounding the raft was removed wide enough to place all the necessary equipment and be able to correctly perform the full-scale horizontal loading test, so that the depth of the excavation was equal to the height of the raft. Therefore, the thickness of the soil surface layer was modified and considered during the numerical simulations.

Regarding the constitutive model used to simulate soil behavior, the elasto-plastic Mohr-Coulomb model was selected. The input data were initiated according to the values shown in Table 1 and adjusted interactively until a best fit was obtained in comparison to the in-situ test results. With respect to the interface between the pile shaft and the surrounding soil, the β method was considered. This method can be used for both cohesive and cohesionless soils. The method is based on effective stress analysis, and is suited for short and long-term analysis of pile load capacity, Helwany, (2007).The contact between the pile tip and soil was considered to be a hard contact according to the software. With regard to the contact between the raft base and the ground surface, a tangential behavior was considered, using a frictional coefficient of 0.15 without shear stress limit, González, (2014).

3. Results and discussion

The maximum horizontal displacement (y) and the ultimate load measured at field (Q_h) resulted in 40.04 mm and 45.50 kN, respectively, while the numerical simulations resulted in 38.58 mm and 44.95 kN. The comparison between the experimental measurements and the numerical simulation is shown in Figure 5, representing an excellent match.

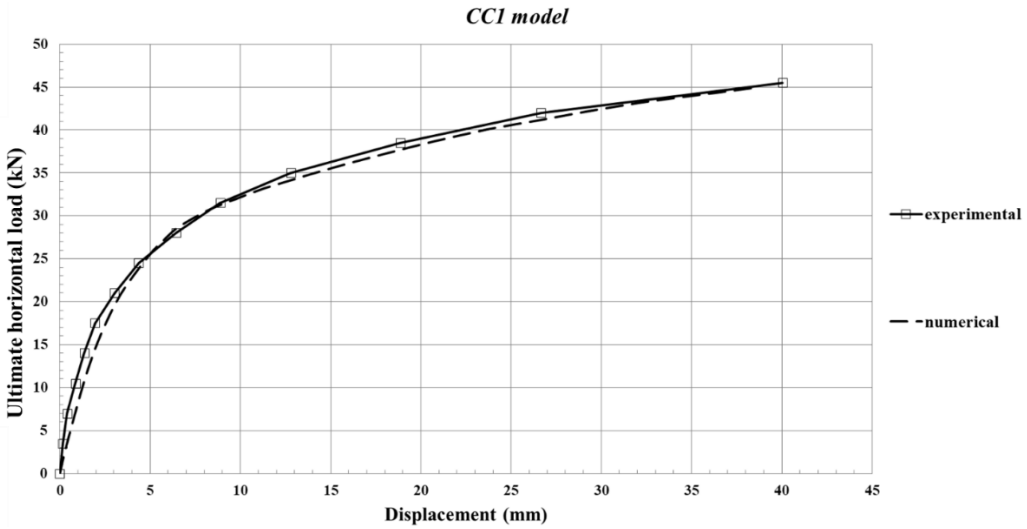

Figure 5. The experimental and numerical results plotted (curve Q_h-y).

Figure 6 shows the 3D graphical results of the horizontal displacements in the same direction as the horizontal loading at the last stage of loading. It is observed the formation of a failure wedge in the front area of the pile (passive zone), and it was evaluated the angle that was formed with respect to the ground surface, which was very close to 45+ø/2 (about 56º), which is the angle of the failure plane according to Mohr-Coulomb criteria.

Table 3 displays the final geotechnical parameters implemented, obtained by successive approximations during the calibration phase. These were increased by 20%, 35%, and 6% for E_s, c and ø, respectively. The parameter f_s indicates the friction stress value used as an interface parameter between the surrounding soil and the shaft of the pile.

Table 3. Final geotechnical parameters used during the numerical analysis.

Final soil parameters for the cc1 piled raft system								
Layer	Thickness (m)	γ_{nat} (kN/m^3)	k_o	E_s (MPa)	v	c (kPa)	ø (°)	f_s (kPa)
1	0.45	14.10	0.40	16.55	0.30	10.00	23.32	2.73
2	1.00	14.20	0.40	13.72	0.30	10.60	22.26	3.78
3	10.55	14.75	0.40	12.00	0.30	18.63	23.32	12.41

The parameters of the soil had the largest influence on the behavior of the foundation system simulated, especially the elasticity soil modulus E_s and the cohesion c; the concrete and steel material had much less influence, but not much less importance. The understanding of the behavior of each one of the materials separately, including their coefficients of variation, it is fundamental, because the range of variations allowed by the material itself helps to significantly decrease some numeric convergence problems and to obtain logical results. According to a numerical sensitivity analysis carried out to obtain acceptable and reliable results, the aforementioned can be affirmed. These statements are supported by the doctoral thesis Alva (2017).

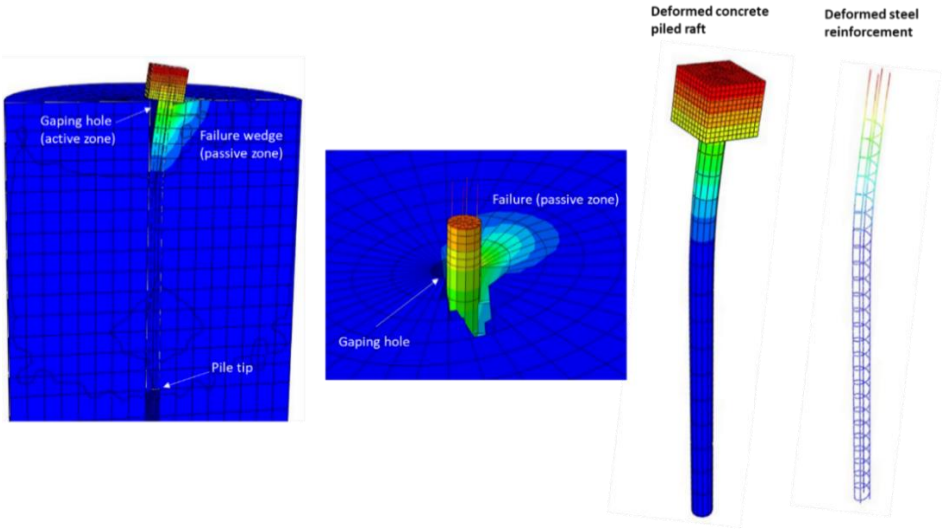

Figure 6. The graphical results in Abaqus software.

Tables 4 and 5 display the concrete and steel parameters adopted during the numerical simulations.

Table 4. Concrete adopted parameters.

Part	γ_c (kN/m^3)	f_{ck} (MPa)	E_c (GPa)	v	*Yield stress compressive* (MPa)	*Yield stress tensile* (MPa)
Raft	21.58	36.70	49.50	0.20	-----	-----
Pile	21.58	36.70	49.50	0.20	40.00	0.873

Regarding both concrete parts, the pile and the raft, an elastic behavior was considered in the raft, whereas an elastic-plastic behaviour in the pile was considered during the numerical modeling to obtain results close to the full-scale test. The constitutive model named concrete damaged plasticity, included in the Abaqus library, requires some input data corresponding to compressive and tensile behavior; both were taken from the concrete manufacturer specifications.

Table 5. Steel adopted parameters.

Part	γ_s (kN/m^3)	E_{steel} (GPa)	f_{yk} (MPa)	v	*Yield stress* (MPa)	*Diameter* (mm)
Rods	77.01	231.00	500.00	0.30	646.80	10.00
Stirrups	77.01	231.00	500.00	0.30	646.80	6.30

It must be clear the behavior of the foundation system occurs as a result of the pile tip, the raft and the pile shaft distribute the external horizontal loading to the soil dominium in different directions at the same time; along the pile shaft two movements happen, first, the shaft pushes against the vertical borehole walls in both positive and negative horizontal directions (subgrade forces); meaning by positive the passive subgrade forces at the top of the pile and by negative subgrade forces at its bottom (also passive forces). In the sequence, a gaping hole appears between the pile shaft and the vertical borehole at the active zone (decompression) at the top of the pile. Simultaneously the piled raft begins to tilt, increasing its contact with the natural ground at the lead side (passive) and decreasing it at the rear side (active). Figure 7 shows a sketch with all this information.

Furthermore, several factors such as soil anisotropy, soil moisture, suction, the current soil stress state, constructive process, etc. are also intrinsically reflected in that curve. All those factors were neither foreseen nor explicitly considered during the numerical simulations, but they were absorbed by the final parameters of the materials assigned during the numerical work, mainly by the soil material. Greater details about this can be found in the doctoral thesis Alva (2017).

The only information summarizes all such factors, displacements and interactions is the Q_h-y experimental curve obtained from the full-scale test, therefore has been important to reproduce that curve numerically the best possible. This is why the soil–structure interaction turned out to be complex to model.

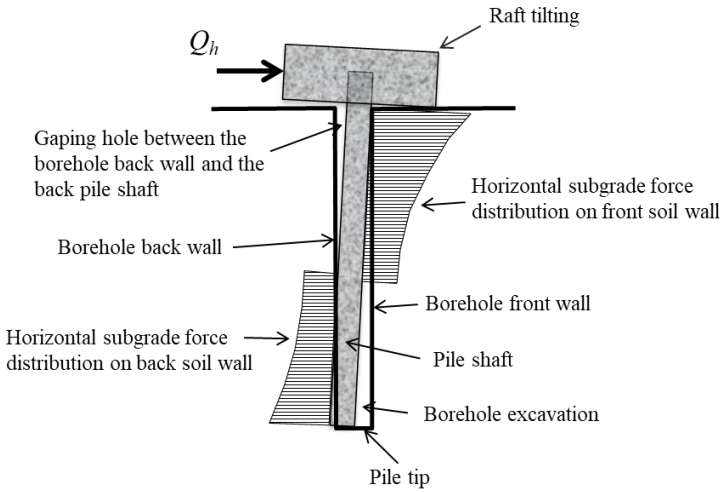

Figure 7. The sketch of the horizontal loading phenomenon. General failure mechanism.

From the numerical curve assessed, the horizontal displacement variation along the pile is shown in Figure 8, and the formation of a plastic hinge at 1.80 m depth is pointed out. It should be noted that each point shown in this chart represents the lateral pile deflection at elevation z when the total horizontal load Q_h has been applied.

Owing to the construction process of the piled raft, the soil imposes displacement constraints along the pile shaft, but those restrictions during the loading test were not strong enough to keep the pile totally fixed to the ground, as can be observed in the same Figure 8. Between the pile tip and the plastic hinge, there are depicted small displacements, almost zero at the pile tip (elevation -5.0m). Regarding the horizontal displacements between the plastic hinge and the ground surface, the largest displacements occurred, and a gaping hole appeared at the active zone.

In general, the soil reaction can be a function of the properties of the pile, the stress-deformation soil relationships, the depth of the point considered, the level of pile displacement, the loading velocity, etc. (Reese and Matlock 1956). But obviously, it is difficult to establish a function that takes into account all these variables, and, moreover, even if such a function is obtained, the resolution of the differential equation of the problem becomes very complex. So the resource for solving the problem is to consider Winkler's simplifying hypothesis, whereby soil reaction p is proportional to displacement y.

A math function $y=f(z)$ was assessed from the experimental curve Q_h-y instead of evaluating the lateral displacements by the differential equation solution. The subgrade soil reaction theory admits that the behavior of a pile subjected to horizontal loading is similar to the behavior of a beam; that is why the beam length axis matchs with the pile length axis in Figure 9.

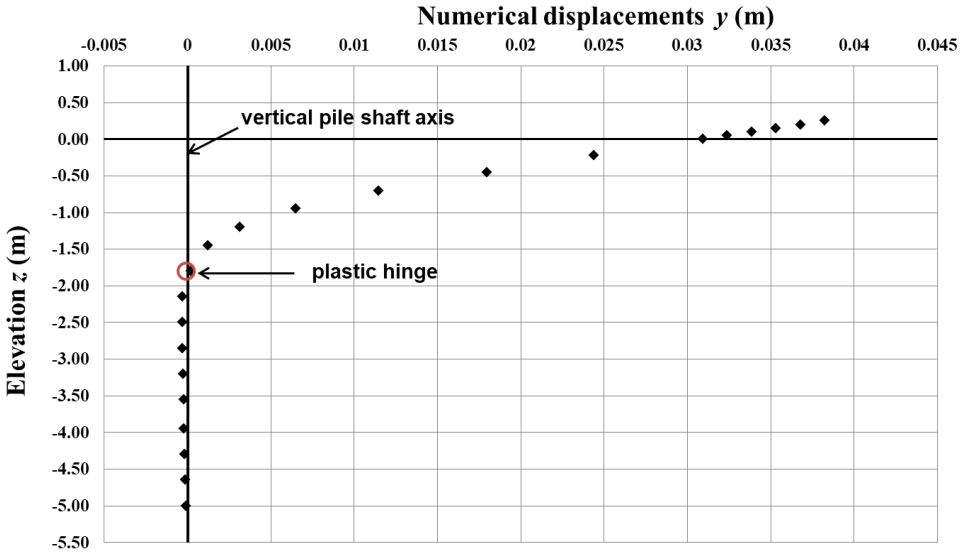

Figure 8. The fitted curve.

The Winkler approach, also called the subgrade reaction theory, is the oldest method for predicting lateral deflections, rotations and stresses in single piles. The behaviour of a single pile can be analyzed using the equation of an elastic beam supported on an elastic foundation, which is represented by the 4th order differential beam bending:

$$E_p I_p \cdot \frac{d^4 y}{dx^4} + K \cdot y = 0 \quad (1)$$

E_p – Modulus of elasticity of the pile; I_p – moment of inertia of the pile section; y – lateral deflection of the pile along the length of the pile; K – Subgrade reaction modulus of soil

Equation 1 represents the soil reaction acting over the pile, or, from a structural point of view, it is the distributed loading over the beam [FL^{-1}].

By means of a multiple regression tool, a polynomial function has been fitted through the displacement points, resulting a sixth degree polynomial function (equation 2), and its coefficient of determination for multiple regression R^2 resulted in 99.984%.

$$y = -0.00006582 \cdot x^6 + 0.00094489 \cdot x^5 - 0.00478857 \cdot x^4 + 0.01078163 \cdot x^3 - 0.01061079 \cdot x^2 + 0.00345756 \cdot x - 0.00017245 \quad (2)$$

By this equation is possible to evaluate the displacements in the concrete pile submitted under the horizontal load in the specific conditions of the experiment carried out. The accuracy of the fitting can be estimated using the root mean squared error (RMSE):

$$RMSE = \sqrt{\sum_{i=1}^{n} (yp_i - yn_i)^2} \quad (3)$$

yn_i - displacements correspond to the numerical simulation results; yp_i - displacements correspond to the polynomial equation.

Once the fitted curve was accepted as quite accurate ($RMSE$=9.01x10^{-4} m), then the polynomial equation was derived successivelly, according to the theory of strength of materials (Timoshenko 1940), to obtain the rotation, the bending moments and finally the shearing force along the pile respectively. Figures 9, 10, and 11 displays those results.

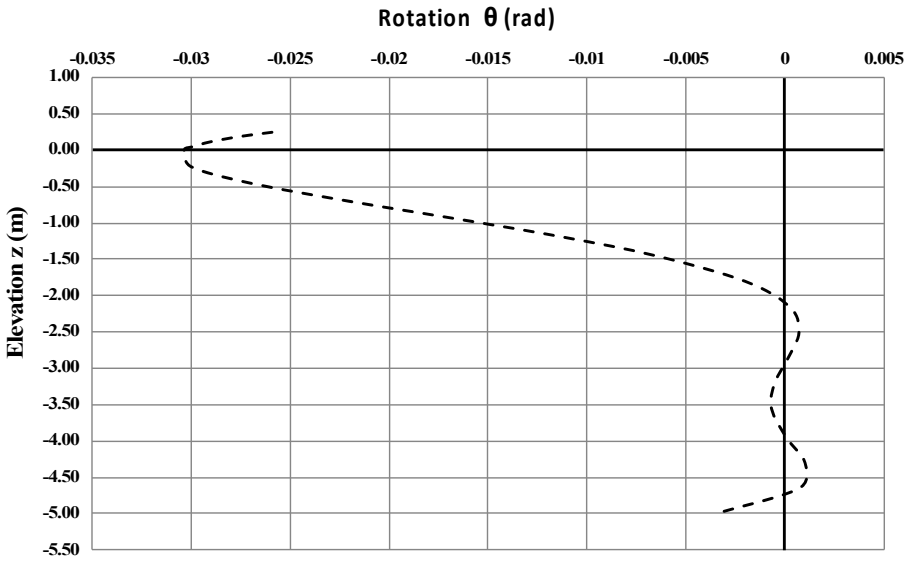

Figure 9. The rotation of the pile.

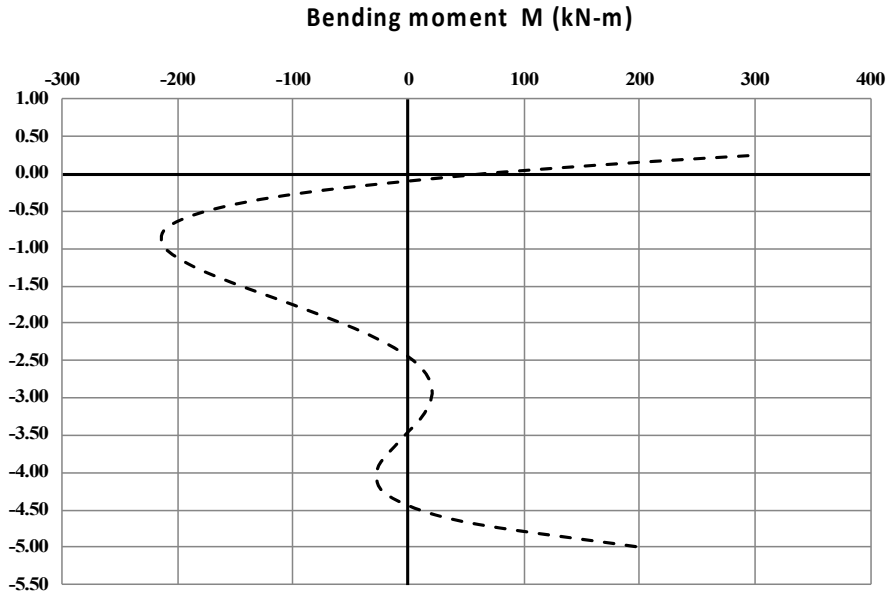

Figure 10. The bending moments in the pile.

The greatest internal bending moments are observed above the plastic hinge located at the elevation -1.80 m. Beneath of this point the values begin to decrease, but at the bottom they increase again; this is due to the evaluation of the polynomial that yielded small displacement values and consequently large values; the same happens with the shearing forces (Figure 11).

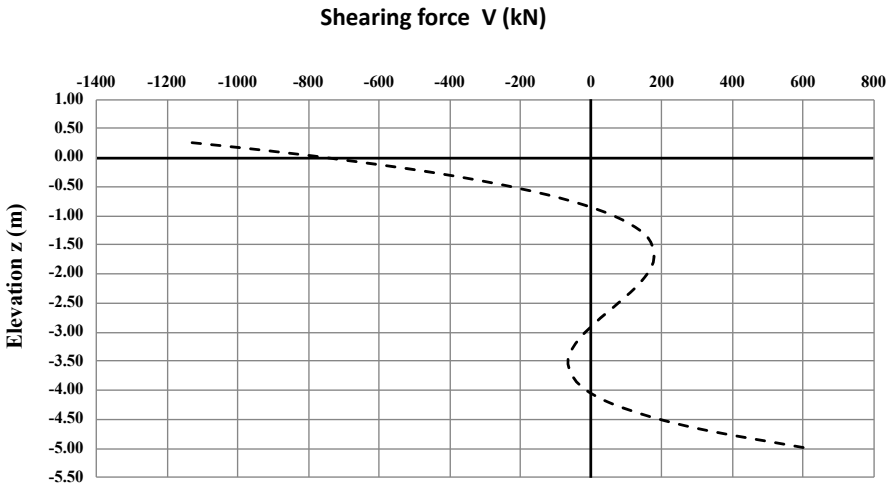

Figure 11. The shearing forces in the pile.

In order to have a sensitivity about the intensity of the loading that the soil receive, several numerical *p-y* curves were obtained during the numerical simulations, but only the curves at 0.0m and -1.0m elevation are depicted in Figure 12; the other curves corresponding to deeper elevations can not be properly observed in the same chart as they have displacements close to zero. Notice that the experimental Q_h-*y* curve (Figure 5) is not drawn in this chart as the magnitude load is out of this particular graphic scale.

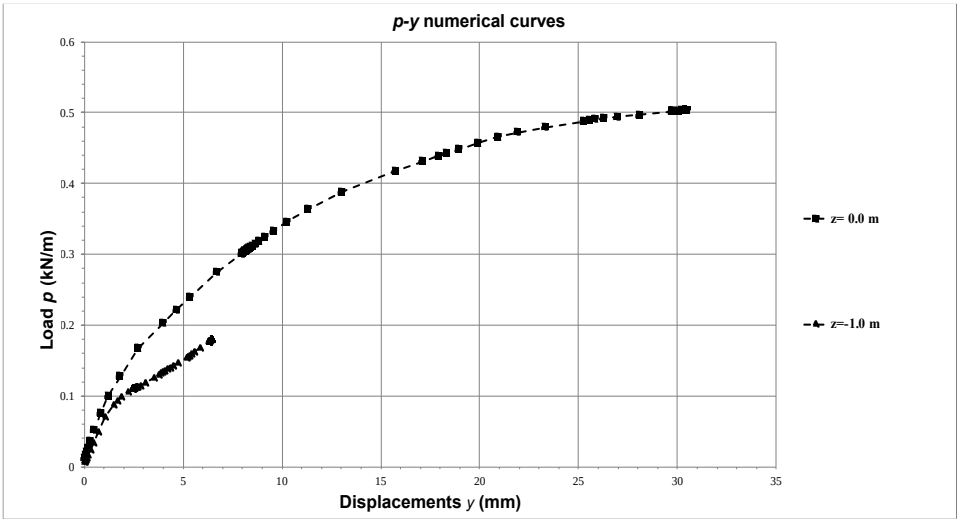

Figure 12. The numerical *p-y* curves obtained at different elevations.

It should be noted that the fourth derivative of equation 2, which results in a power 2 polynomial, does not represent the actual loading distribution acting over the pile, because such an equation was assessed from the numerical pile displacements. Therefore, it was essential to calculate the soil reaction over the pile using Winkler's equation ($p=Ky$), to represent the actual load intensity over it, as shown in Figure 7. It is important to mention that to assess the modulus *K*, the numerical results provided both the horizontal displacements and the normal reaction forces of the soil over the pile at both walls of excavation. Those lateral displacements resulted lower than those obtained straight from the pile.

The soil reaction forces *p* at any depth *z* acting in opposite direction to pile deflection and at the same depth on the walls of the excavation; however, they are plotted as positive in Figure 13.

Moreover, from the SPT field data (Figure 1), the subgrade reaction modulus is calculated by theTerzaghi's expression for sands (equation 4) as:

$$K = \frac{C \cdot \gamma}{1.35} \cdot z \tag{4}$$

γ - unit weight; z - depth in the soil; C is a coefficient evaluated by:

$$C = \left[\frac{N_{SPT}}{0.5+0.015 \cdot N_{SPT}}\right]^2 + 80 \tag{5}$$

This SPT curve assessed represents the subgrade reaction modulus variation of the excavation, whereas, numerically were obtained two curves, one corresponding to the front wall and the other to the back soil wall of the excavation. This seems more realistic, since soils have different stiffness under the active and passive lateral pressures. The Terzaghi's criteria is also shown in Figure 14 only as reference.

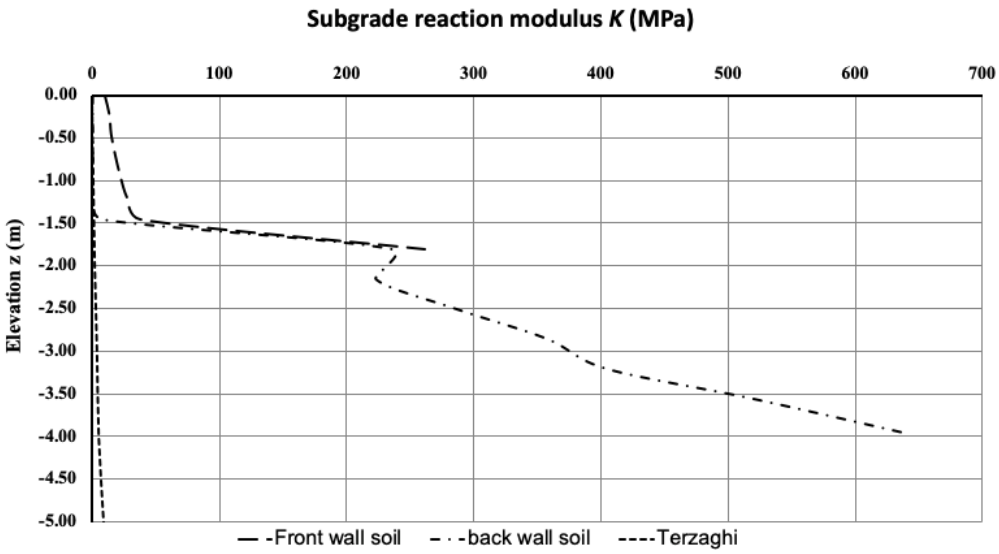

Figure 13. The subgrade reaction modulus versus depth.

Taking the *K* values previously assessed, the acting load along the pile has been evaluated and plotted as shown in Figure 14. The loading intensity *p* is negative because it is acting opposite to the displacements direction over the front shaft pile, whereas over the back shaft pile also results in negative because the displacements resulted in a numerical negative direction, although he loading intensity has a positive direction. Also it is observed in this chart the gap formation between the pile and back soil wall begins at the elevation -1.0 m.

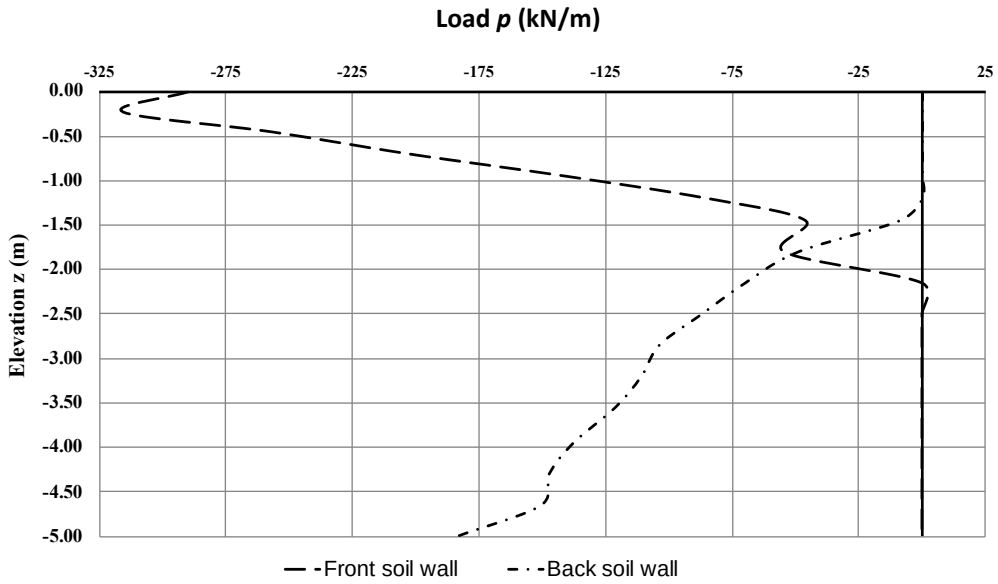

Figure 14. The loading intensity over the pile.

4. Conclusions

A 3D simulation of the behavior of a piled raft with a single pile has been studied, and interesting conclusions have been drawn regarding the structural behavior and the response of the soil involved in 3D numerical nonlinear analysis. The following conclusions are listed:

1. The numerical works through the FEM resulted succesful according to the graphical results, considering the elastoplastic behavior both the pile as in the soil.
2. The Mohr-Coloumb constitutive soil model was enough to represent the behaviour of the soil dominum during the loading process, even though the installation of the pile was not modeled.
3. It was fundamental to consider the elastic-plastic behavior in the concrete material during the numerical modeling for obtaining results close to the full-scale test.
4. The math function obtained represents exclusively the mechanical behaviour of the foundation system here studied.
5. The most relevant displacements and internal forces in the pile appeared above the plastic hinge, corresponding to soil influenced in 1.80 m depth beneath from the natural ground level (roughly 7 times the diameter of the pile).
6. The graphics of rotation, bending moment and shear force, were evaluated from the numerical pile displacements, while the loading intensity over the pile was evaluated from both the horizontal displacement and normal reaction forces of the soil using Winkler's equation.
7. The lateral displacements calculated both in the pile and the excavation walls did not result in equals, although the theoretical solution considers them equals. Also, in the numerical model, a frictional contact constraint between the pile and the surrounding soil was considered. Both reasons explain some of the differences in the shape of the curves evaluated with respect to those in Figure 1.
8. The modulus reaction varies differently in both excavation walls according to the numerical analysis; this scenario seems more realistic than the single curve given by Therzaghi´s equation, since soils have different stiffness under loading and unloading conditions.
9. It is possible to study other hypothetical cases by only changing in the numerical model developed the diameter and length of the piled raft as well as the magnitude, position, and direction of the loading. They are not presented in this paper.

10. If, in this numerical model, changes are made in the soil properties as well as in the geometry and material of the pile, for instance, a steel pile with a non-circular cross-section in clay soil, the results will yield a crude prediction of the behavior of such a foundation system. Therefore, it is not recommended to implement this numerical model to evaluate other studies.

According to the results here presented, it can be cited as follows: “The prediction of a single pile response is still a fundamental step in the design process, but it is also uncertain”(Mandolini 2019).

Some possible paths of interest that could be explored include the following:

- To carry out some parametric studies on the same piled raft changing loading direction and loading magnitude.
- To change the diameter and the length of the pile.
- To increase the number of piles in the system could be another option.

Author contributions: Author 1: Conceptualization, methodology, experimental investigation, drafting, review and supervision and enhancement of manuscript. Author 2: Methodology, review and supervision, enhancement of manuscript. Author 3: Methodology, review and supervision, enhancement of manuscript.

Funding: This work was supported by the Brasilia University.

Acknowledgments: We would like to express gratitude to the Brasilia University for supporting this research.

Conflicts of interest: The authors declare no conflict of interest.

References

Abaqus. (2019). Documentation Collection, Analysis User´s Manual.

Abdel-Azim, O. A., K. Abdel-Rahman, and Y. M. El-Mossallamy. (2020). Numerical Investigation of Optimized Piled Raft Foundation for High-Rise Building in Germany. *Innovative Infrastructure Solutions* 5(1),1-11. doi: 10.1007/s41062-019-0258-4.

ABNT-Brazilian National Technical Standards Association. (2006). NBR 12131: Piles - Static Load Test - Method of Test.

Alva, F. (2017). Analysis of the Behavior of Piled Rafts with and without Defective Pile Horizontally Loaded in Tropical Soil. (PhD Thesis, University of Brasilia, Brasilia, Brasil).

André de Almeida, M., M. G. Miguel, and S. H. C. Teixeira. (2011). Horizontal Bearing Capacity of Piles in a Lateritic Soil. *Journal of Geotechnical and Geoenvironmental Engineering* 137(1), 59–69. doi: 10.1061/(ASCE)GT.1943-5606.0000410.

Deb, P., and S. K. Pal. (2019). Numerical Analysis of Piled Raft Foundation under Combined Vertical and Lateral Loading. *Ocean Engineering* 190(June),106431. doi: 10.1016/j.oceaneng.2019.106431.

García, F. J. A., Y. Machado, M. M. Farias, and R. M. Cabral. (2020). Modelagem Numérica Da Fundação de Um Protótipo Eólico Submetida a Carregamento Horizontal Monotônico. *Congresso Brasileiro de Mecânica dos Solos e Engenharia Geotécnica*, 2350–2359, ABMS.

Gon, F. (2011). Geotechnical Characterization by Testing Laboratory Tests of a Diabase Soil from Campinas Region of Campinas/SP. (MSc. Thesis, University of Campinas, Campinas, Brasil).

González, J. (2014). Numerical Behavioral Study of Lateral Loading Piles.(MSc. Thesis, University of Brasilia, Brasilia, Brasil). [in Portuguese].

Helwany, S. (2007). *Applied Soil Mechanics with ABAQUS Applications*. Jhon Wiley and Sons Inc.

Jeong, S., J. Park, and D. Chang. (2024). An Approximate Numerical Analysis of Rafts and Piled-Rafts Foundation. *Computers and Geotechnics* 168(January),106108. doi: 10.1016/j.compgeo.2024.106108.

Kim, Y., S. Jeong, and S. Lee. (2011). Wedge Failure Analysis of Soil Resistance on Laterally Loaded Piles in Clay. *Journal of Geotechnical and Geoenvironmental Engineering* 137(7), 678–94. doi: 10.1061/(asce)gt.1943-5606.0000481.

Mandolini, Alessandro. (2019). Lessons Learned from Experimental Researches on Piles – A Personal Point Of View. *4° Congreso Internacional de Fundaciones Profundas de Bolivia*, edited by B. H. Fellenius, K. R. Massarsch, A. Mandolini, M. T. A., and M. T. Herrera. Santa Cruz de la Sierra.

Patil, J. D., S. A. Vasanvala, and C. H. Solanki. (2013). A Study on Piled Raft Foundation: State of Art. *International Journal of Engineering Research and Technology* 2(8),1464–1470.

Reese, C., and W. Van Impe. (2001). *Single Piles and Pile Groups under Lateral Loading*. 2nd ed. CRC Press.

Reese, L. C., and H. Matlock. (1956). Non-Dimensional Solutions for Laterally-Loaded Piles with Soil Modulus Assumed Proportional to Depth. *8th Texas Conference on Soil Mechanics and Foundation Engineering*, 1–41. Austin, Texas.

Stacul, S., N. Squeglia, and F. Morelli. (2017). Laterally Loaded Single Pile Response Considering the Influence of Suction and Non-Linear Behaviour of Reinforced Concrete Sections. *Applied Sciences (Switzerland)* 7(12). doi: 10.3390/app7121310.

Sümer, Y., and M. Aktaş. (2015). Defining Parameters for Concrete Damage Plasticity Model. *Challenge Journal of Structural Mechanics* 1(3), 149–155. doi: 10.20528/cjsmec.2015.07.023.

Timoshenko, S. (1940). *Strenght of Materials Part I and II*. 2nd ed. New York: Van Nostrand Company, Inc.